

## On the Contact Characteristics between Droplet and Microchip/Binding Site for Self-Alignment

Wen-Hwa Chen<sup>1,2</sup> and Tsung-Yu Huang<sup>1</sup>

**Abstract:** The contact characteristics between a droplet and a microchip/binding site strongly affect the accuracy of self-alignment in the self-assembly of micro-electronic-mechanical systems. This study is mainly to implement the Surface Evolver Program, which is commonly adopted for studying surface shaped by surface tension and other energies, to investigate comprehensively the contact characteristics between the small droplet and the microchip/binding site. The details of changes in the contact line and the contact area when the microchip is subjected to translation, compression, yawing and rolling are drawn. The three-dimensional deformation of the droplet between the microchip and the binding site is also presented. The restoring force and restoring torque that are induced on the microchip under those motions are calculated accurately. The critical value that the microchip can return to its aligned position under respective motion is therefore predicted. Lastly, under the effects of the droplet surface tension and the contact angle for the droplet on the microchip/binding site, the regions of overflow and no wet area on different microchip shapes are demonstrated. The computed results agree excellently with those by experiments. Based on the simulation techniques developed, the self-alignment of the microchip with the binding site can be estimated accurately.

**Keywords:** Self-alignment, Surface Tension, Surface Evolver Program, Contact Line, Contact Area, Restoring Force, Restoring Torque.

### 1 Introduction

In recent years, the development of precise assembly technology in micro-electro-mechanical systems (MEMS) has been widely applied to assemble micropart for modern electronic devices. Among those, the self-alignment of micropart by using

---

<sup>1</sup> Dep. of Power Mech. Engng., National Tsing Hua University, Hsinchu, Taiwan, R.O.C.

<sup>2</sup> National Applied Research Laboratories, Taiwan, R.O.C.

liquid surface tension has particularly great potential for practical applications, and therefore becomes the main aim of this work to tackle.

Numerous experimental studies of the self-alignment of the micropart with a binding site have been published. Sato *et al.* (1999) designed an experiment to investigate the initial alignment of a square micropart with the binding site using the surface tension of a water droplet. The alignment characteristics that were governed by the wettable surface of the micropart and the binding site were examined. The experimental results revealed a misalignment of under  $10\mu\text{ m}$ . Srinivasan *et al.* (2001) performed the self-alignment experiments for different shapes of microparts, including a twenty-gon (approximately circular), square, rectangle, regular hexagon, semicircle and comma (like a meniscus). The twenty-gon and square gave a better alignment precision than those of the other shapes. Sato *et al.* (2003) developed an experiment on self-alignment under the surface tension of water droplet using other microparts with shapes, including a cross, star, triangle and hexagon. They demonstrated that the water droplet overflowed a micropart/binding site and the area near the corner was never wet, regardless of the pattern. These effects may cause the alignment inaccurate. Tsai *et al.* (2007) explored the surface tension of a droplet and the edge effect to perform an experiment on the self-alignment of a microchip. They used the protrusion of the binding site to replace the hydrophilic and hydrophobic interfacial surfaces on the plane. The misalignment of the experiment was less than  $16\mu\text{ m}$ .

With respect to simulations of self-alignment or self-assembly, Zhu *et al.* (1998) applied the Surface Evolver Program (Brakke, 1996) to calculate the restoring force when a chip was mismatched with a substrate on flip-chip packaging. It was found that as the solder volume decreases or misalignment grows, the restoring force increases. Böhringer *et al.* (2001) employed the MATLAB program to calculate the minimum and maximum global and local energies. They predicted that floating substrates would be found at the maximum of local energy. This prediction was consistent with the experiment of Srinivasan *et al.* (2001). Other research involved placing a self-alignment system in water and predicting the precision of alignment. Greiner *et al.* (2002) utilized the Surface Evolver Program to calculate the restoring force, restoring torque and potential energy when a droplet was under extension or compression, or while a micropart was under translation or rotation. However, the analyzed droplet volumes,  $50\text{ nl}\sim 150\text{ nl}$ , were too large to discuss the change of the contact line. The deformation of the droplet could not be described well at the corners and boundary of the micropart/binding site. Therefore, studies of smaller droplets would be very valuable. Sato *et al.* (2003) made some assumptions and established a simplified model to analyze the self-alignment of the microchip with the binding site. Since the assumptions in the simplified model differed from practical

contact characteristics, further studies on the contact characteristics between the droplet and the microchip/binding site for self-alignment should receive attention. Kim *et al.* (2004; 2005) also employed the Surface Evolver Program to compute the restoring force resulting from the surface tension of a droplet. They demonstrated that the restoring force was generated by resin or solder droplet when the micropart and the binding site were misaligned and a larger misalignment was associated with a larger restoring force. Berthier *et al.* (2010) derived an approximate model to calculate the restoring force, restoring torque and potential energy when a droplet was under extension or compression, or while a micropart was under translation or rotation. Those calculated results were compared with that by the model using the Surface Evolver Program. However, the same problem encountered as that by Greiner *et al.* (2002), the analyzed droplet volumes, 250nl~2500nl, and the microchip sizes, 5mm, were too large to study the change of the contact characteristics.

A number of studies discussed the deformation of droplet using Surface Evolver Program. Chen *et al.* (2005) investigated the solder bridging before and during the reflow process in electronic packaging. They discussed several factors that affect the shape of solder bridging, including the pad size, the pitch between adjacent pads, the contact angle between the solder and the pad/mask, the surface tension and volume of the solder. The developed model can be practically applied to predict the stability of solder bridging. Lin *et al.* (2007) explored the formation of the solder ball in a BGA package. The comparison of influence factors in Surface Evolver and Heinrich models was discussed, such as the pad radius, the surface tension of the solder ball, the contact angle of the solder ball on the pad and the stand-off height during the reflow process. Some researches further explored the surface tension and contact angle of the droplet. For example, Xie *et al.* (2007) used the Moving Particle Semi-impact (MPS) method to simulate the shape of the droplet. However, the alignment of the microchip with the binding site and the contact characteristics for small volume of droplet in three dimensions have rarely been discussed.

In this study, the Surface Evolver Program is applied to analyze not only the three-dimensional deformation of the droplet between a microchip and a binding site, but also the contact characteristics, like the contact line, contact area, overflow and no wet area. Other factors that will influence the deformation of the droplet, such as the radius of curvature, surface tension and gravity, are also discussed. The computed results are useful in determining the parameters, including the surface tension of droplet, droplet volume and wettability of interfaces, to improve the accuracy of self-assembly or self-alignment.

## 2 Self-alignment

Since micro-components in a micro system are small, aligning or assembling them is difficult. Some slight deviations in alignment can cause the system to short circuit or burnout, thereby becoming useless. Additionally, such components cannot be controlled by a pick-and-place method. To increase the usability of a micro system, the accuracy of self-alignment of micro-components must be improved and maximized. Accordingly, with reference to some applications of flip-chip technique (Lo *et al.*, 2008) or RFID microchip packaging (Tsai *et al.*, 2007), the possible self-alignment of the microchip under the effects of restoring force or restoring torque between pad and solder warrants discussion. Besides, the precision of the self-alignment of the microchip with the binding site also depends on the deformation of the droplet. These factors are closely related to the surface tension of the droplet, and its contact angle on the microchip or the binding site, as well as the distribution of the contact line and the contact area.

### 2.1 Surface Tension and Contact Angle

The surface tension of the droplet is the force that is exerted on surface molecules to keep the molecules together along the surface. The surface tension is always cohesive. Therefore, as surface tension of the droplet increases, the cohesion increases. In general, the droplet surface tension is related to the surrounding temperature. As the ambient temperature increases, the cohesion and surface tension decrease. This study discusses the formation of the droplet under isothermal conditions, such that the effect of temperature is ignored here.

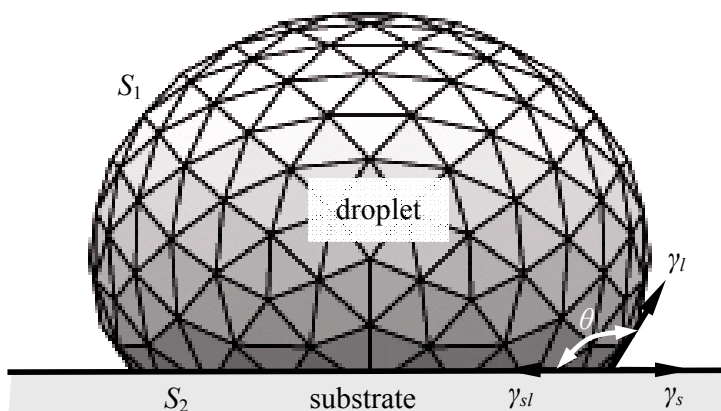


Figure 1: The formation of a droplet on a substrate

When the droplet condenses steadily on the smooth surface of a substrate, the an-

gle between the surface tension  $\gamma_l$  of the droplet along the tangent direction of its curved surface and the tension  $\gamma_{sl}$  at the interface between the substrate and droplet is called the contact angle  $\theta$ , as seen in Fig.1. Whereas the surface tension  $\gamma_l$  would cause the droplet to condense on the substrate, the interfacial surface tension  $\gamma_{sl}$  shrinks the contact area with the substrate. Another interfacial surface tension  $\gamma_s$  between the air and the substrate resists the shrinkage of the contact area. Based on the force balance, the relationship among the interfacial tensions  $\gamma_l$ ,  $\gamma_{sl}$  and  $\gamma_s$  and the contact angle  $\theta$  is given by Eq. (1),

$$\cos\theta = \frac{\gamma_s - \gamma_{sl}}{\gamma_l}. \quad (0^\circ \leq \theta \leq 180^\circ) \quad (1)$$

Equation (1) is also called Young's equation (Myers, 1999). When the contact angle  $\theta$  is less than  $90^\circ$ , the surface is wettable. When the contact angle  $\theta$  exceeds  $90^\circ$ , the surface is non-wettable. If the contact angle  $\theta$  equals or approximates  $0^\circ$ , then the surface is completely wettable. If the contact angle  $\theta$  equals or approaches  $180^\circ$ , then the surface is completely non-wettable.

## 2.2 Contact Line and Contact Area

When the droplet surface tension  $\gamma_l$ , the interfacial surface tension  $\gamma_{sl}$  between the droplet and the substrate, and the interfacial surface tension  $\gamma_s$  between the air and the substrate are on force balance, the contact line and the contact area are formed. Since the interfacial surface tension  $\gamma_s$  between the air and the substrate is constant, the contact line and the contact area are affected by the droplet surface tension  $\gamma_l$  and the interfacial surface tension  $\gamma_{sl}$ . The contact area of the interfacial surface tension  $\gamma_{sl}$  existing between the droplet and the substrate is also called the wetted area.

On the micro-scale, the effect of the surface tension of the droplet and the interfacial surface tension is important for the formation of the droplet (Yang *et al.*, 2006). Each corner of the microchip or the binding site is difficult to fill with a droplet, and the cohesion of the droplet forms no wet area in the corner due to the surface tension of the droplet, especially when the microchip or the binding site is not circular. When the microchip and the binding site are misaligned, the shape of the contact line and the contact area between the droplet and the microchip or the binding site is affected. Therefore, the restoring force and restoring torque are changed further.

The volume of the droplet is another important factor that influences the shape and location of the contact line and the contact area, changing the magnitude of the restoring force or the restoring torque. If the droplet is too large, the microchip yaws or rolls easily. If the droplet is too small or the microchip rolls too serious,

the microchip may come into contact with the binding site. Therefore, the selection of the droplet with suitable volume warrants further study.

### 3 Surface Evolver Program

The Surface Evolver Program is based on the principle of minimum total potential energy to analyze the formation and evolution of the boundary of droplets in three dimensions. In calculations using the Surface Evolver Program, the surface of a three-dimensional droplet is firstly meshed into triangular facet elements, as shown in Fig.1. Then, the program continuously utilizes iterative methods to calculate the total energy of all triangular facet elements. Each size and location of the triangular facet elements are changed gradually, until the total energy of the droplet reaches its minimum. Finally, the final contour of the droplet in the steady state is determined. The Surface Evolver Program can analyze the effect of surface tension and gravity subjected to some constraints, such as the droplet that is deposited on a solid surface will not penetrate into the solid; the volume of the droplet that is covered by facet elements equals a pre-specified value; the contact angle between the droplet and solid is prescribed, or the interfacial surface tension of the droplet is fixed.

Generally, the total energy of the droplet consists of the surface tension energy  $E_{surface\ tension}$ , the gravitational potential energy  $E_{gravity}$  and the potential energy associated with other external forces. For a droplet to which no external force is applied, any corresponding potential energy can be ignored. Accordingly, the total energy  $E$  is given by

$$E = E_{surface\ tension} + E_{gravity}, \quad (2)$$

and the surface tension  $E_{surface\ tension}$  of the droplet is

$$E_{surface\ tension} = \iint_{S_1} \gamma_l dA + \iint_{S_2} \gamma_{sl} dA, \quad (3)$$

where  $S_1$  is the surface of the droplet that is covered with a curved surface, which comprises a set of triangular facet elements.  $S_2$  is the interfacial surface between the droplet and the substrate. The gravitational potential energy of droplet  $E_{gravity}$  is given by

$$E_{gravity} = \iiint_{\Omega} dV, \quad (4)$$

where  $\Omega$  is the body domain of the droplet.

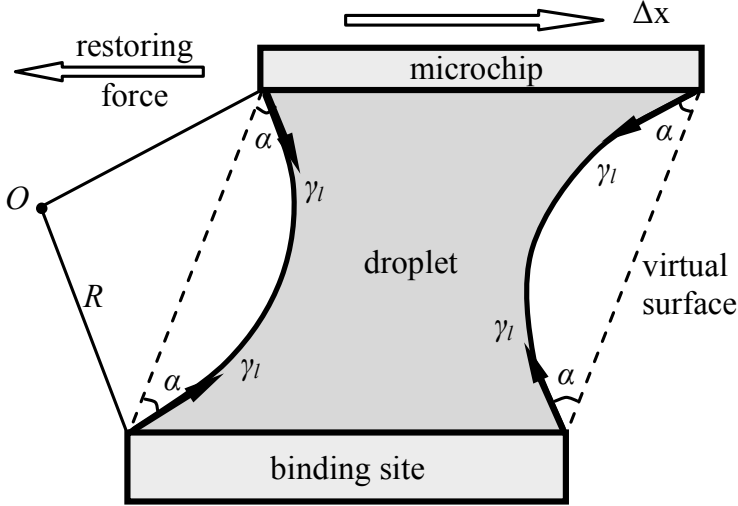


Figure 2: The Sato's simplified model for the self-alignment of the microchip with the binding site

#### 4 Results and discussion

Fig.2 shows the Sato's simplified model (Sato *et al.*, 2003), which makes assumptions to analyze the self-alignment of the microchip with the binding site subjected to a translation. Sato *et al.* (2003) assumed that the radius of curvature of the droplet  $r$  is uniform. In addition, the contact line coincides with the side boundary of the microchip/binding site. These lead to an equivalent two-dimensional analysis model. Besides, all the  $\alpha$  angles between the direction of the droplet surface tension  $\gamma_l$  and the virtual surface of the parallelogram at four corners are assumed to be equal to each other. This differs from practical reality. The contact behaviors among the droplet, the microchip and the binding site therefore cannot be correctly described and will increase the errors for computing the restoring force. Moreover, the two-dimensional analysis model cannot properly represent the bulging and concave surface on each cross-section, especially at four corners of microchip/binding site. The regions of no wet area at four corners of microchip/binding site are therefore not sketched accurately.

The Surface Evolver Program is thus applied to study the self-alignment of the microchip with the binding site. The deformation of the droplet, the contact line and the contact area, and the calculation of the restoring force or the restoring torque

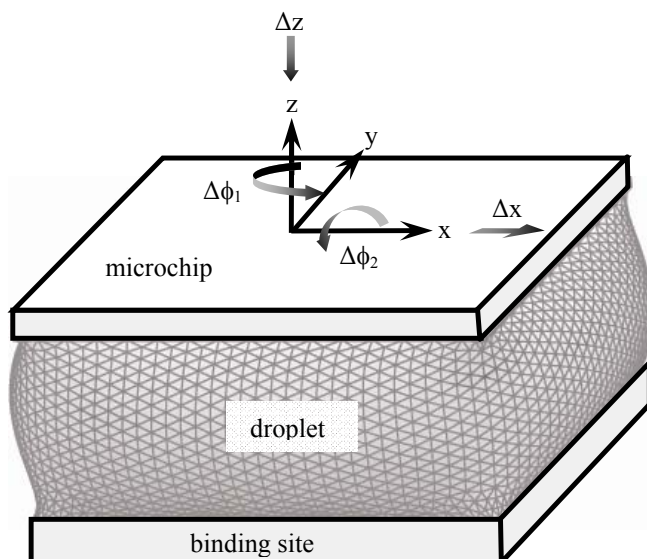


Figure 3: The present model for the self-alignment of the microchip with the binding site

of the microchip are performed. The movements of the microchip considered were the translation  $\Delta x$ , compression  $\Delta z$ , yawing  $\Delta\phi_1$  and rolling  $\Delta\phi_2$  (see Fig.3), which greatly demonstrate the accuracy of self-alignment of the microchip with the binding site. The overflow and no wet area when the droplet is deformed by various shapes of microchips can also be noted.

#### 4.1 Square microchip and binding site

To compare with the analytic and experimental results of Sato *et al.* (2003), the area  $800 \times 800 \mu\text{m}^2$  of the square microchip and binding site of size  $1000 \times 1000 \mu\text{m}^2$  is selected for study herein. The related parameters adopted in Sato *et al.* (2003), such as the contact angle, the surface tension and density of water droplet and the weight of the microchip are also taken in this study. The three volumes of the droplets are 12nl, 23nl and 35nl. The area  $800 \times 800 \mu\text{m}^2$  of the binding site is wettable or hydrophilic; the left area of the binding site is non-wettable or hydrophobic (Sato *et al.*, 2003).

Since the initial contact between the droplet and the microchip/binding site is incomplete when the microchip is falling under gravity, the contact area does not



cover the entire surface of the microchip or the binding site. The contact area increases gradually as the height of the droplet decreases due to the falling of the microchip. The droplet deforms to an equilibrium shape, and the height of the microchip is its static height  $z_0$  (Böhringer *et al.*, 2001). For the droplet with volume 23nl, for example, the static height  $z_0$  calculated by the Surface Evolver Program in this study is  $35.97\mu\text{m}$ . The result agrees very well with the Sato's experimental data,  $z_0 = 36\mu\text{m}$  (Sato *et al.*, 2003). It reveals the accuracy of the computation model proposed herein using the Surface Evolver Program. By the present model, the static heights  $z_0$  of the droplets with the volumes of 12nl and 35nl are  $18.75\mu\text{m}$  and  $54.86\mu\text{m}$ , respectively.

#### 4.1.1 Translation

Based on the static height of the droplet  $z_0$ , this study first analyzes the self-alignment of the microchip with the binding site subjected to a translation  $\Delta x$  of the microchip. As expected, due to the effect of the surface tension of droplet  $\gamma_l$ , the horizontal restoring force  $F_x$  gradually increases with the translation  $\Delta x$ , as seen in Fig.4. Since the Sato's simplified model is limited to the two-dimensional analysis, the contact line and the contact area between the droplet and the microchip/binding site are the same in y-direction (see Fig.3). Therefore, as the translation  $\Delta x$  exceeds  $60\mu\text{m}$  for the droplet with the volume of 23nl or 35nl, the horizontal restoring force  $F_x$  computed by the Sato's simplified model is independent of the translation  $\Delta x$  and remains a steady value. In this situation, the surface tension of the droplet  $\gamma_l$  will be parallel to the planes of the microchip/binding site and violates the physical behaviors.

When the translation  $\Delta x$  is less than  $30\mu\text{m}$  or  $60\mu\text{m}$ , the horizontal restoring force  $F_x$  obtained by the present three-dimensional analysis model does not differ from the Sato's simplified model for the droplet with the volume of 23nl or 35nl, respectively. As the translation  $\Delta x$  exceeds  $30\mu\text{m}$  or  $60\mu\text{m}$  for the droplet with the volume of 23nl or 35nl, however, the results of the present model continuously increase and are larger than those of the Sato's simplified model. As the droplet with volume 12nl, as seen in Fig.4, the horizontal restoring force  $F_x$  by the present model increases slowly and reaches its maximum when the translation  $\Delta x$  approaches  $64.8\mu\text{m}$ , which is called the critical translation  $\Delta x_c$ . It is noted that the critical translation physically indicates the restoring capability for the alignment of the microchip. Droplets with volumes 23nl and 35nl exhibit the same tendency, and their critical translations  $\Delta x_c$  are  $102.4\mu\text{m}$  and  $165\mu\text{m}$ , respectively. Fig.5 presents the three-dimensional deformation of the droplet of volume 35nl at its critical translation  $\Delta x_c = 165\mu\text{m}$ . For clarity, the side view and top view are also shown.

The shape of the contact line and the contact area on the microchip and the bind-

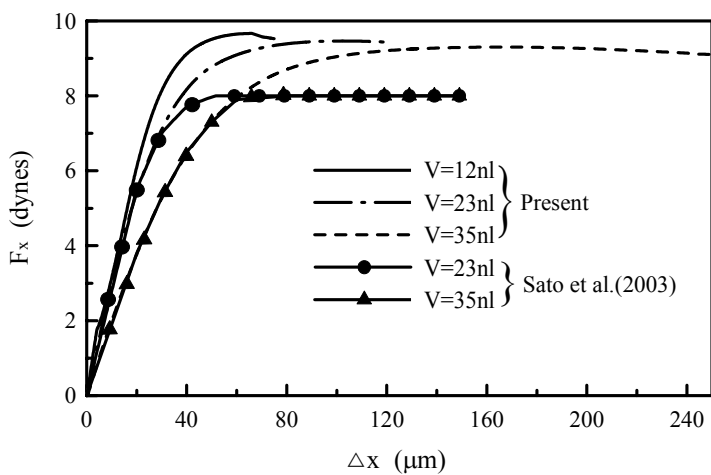


Figure 4: The calculated horizontal restoring force  $F_x$  versus the translation  $\Delta x$

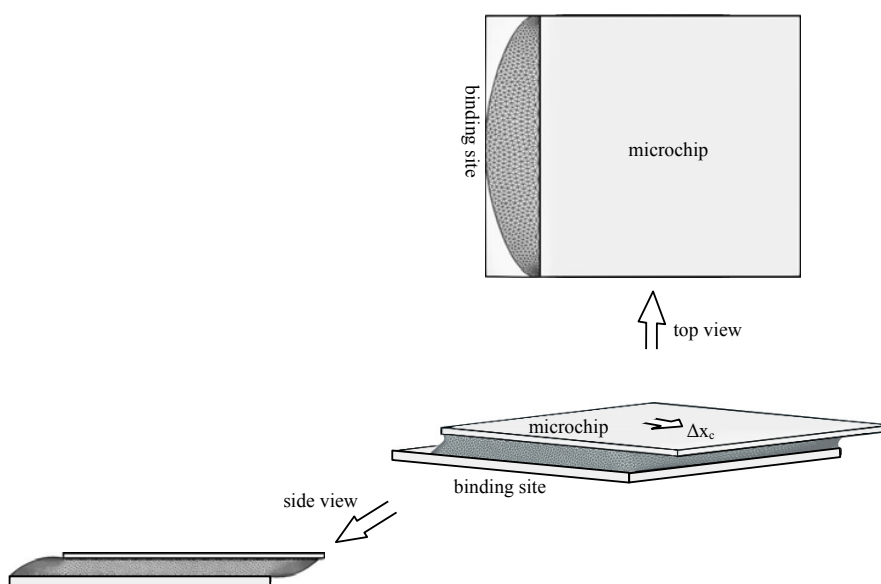


Figure 5: The deformation of the droplet at the critical translation  $\Delta x_c = 165 \mu\text{m}$  ( $V = 35 \text{ nl}$ )

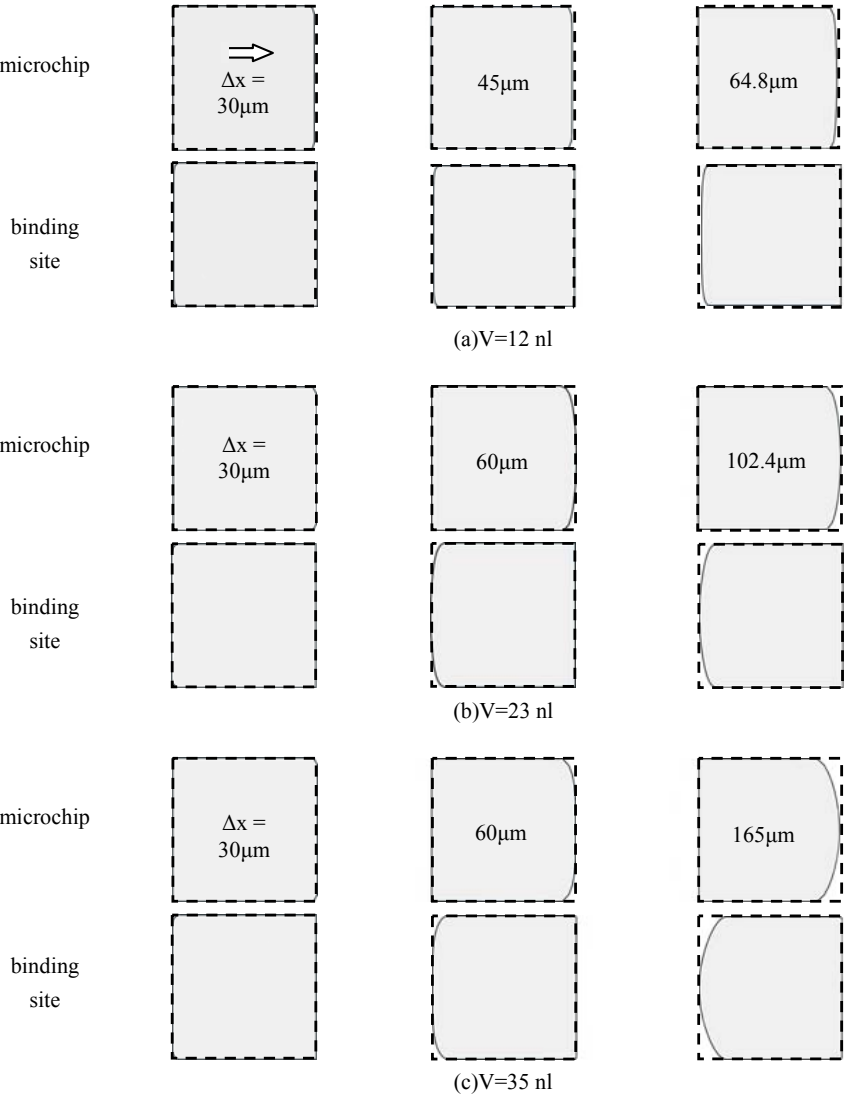


Figure 6: The contact line and the contact area on the microchip or the binding site at various translations  $\Delta x$  of the microchip (---Sato et al. (2003); —present)

ing site also varies with the horizontal restoring force  $F_x$ , affecting the accuracy of alignment (Sato *et al.*, 2003). In Fig.6, the dashed line represents the droplet boundary that was assumed by Sato *et al.* (2003), and the boundary coincides with the sides of the microchip or the binding site. The gray area and the solid line on

the microchip or the binding site represent the contact line and the contact area obtained in this study by the Surface Evolver Program. As the translation of the microchip  $\Delta x$  increases, the difference between the present model and that by Sato *et al.* (2003) becomes more obvious - especially at the corners and the sides of the microchip or the binding site. Consider for example a droplet of volume 12nl, shown in Fig.6 (a): when the translation  $\Delta x$  is  $30\mu\text{m}$ , the contact line on the bottom plane of the microchip starts to move away the right-hand side of the microchip or the contact line on the upper plane of the binding site moves away the left-hand side of the binding site. As the translation  $\Delta x$  increases, the contact line moves distinctly away from the sides of the microchip or the binding site. The maximum translation  $\Delta x_c$  associated with the restoring alignment of the microchip is  $64.8\mu\text{m}$ , and the distribution of the contact line on the microchip and the binding site can then be seen in Fig.6(a). For the droplet with volumes 23nl or 35nl, when the microchip undergoes maximum translation  $\Delta x_c$  of  $102.4\mu\text{m}$  or  $165\mu\text{m}$ , respectively, the contact line moves as shown in Fig.6 (b) and (c). The contact lines move away especially from the corners of the microchip and the binding site. If the microchip does not move more than the critical translation  $\Delta x_c$ , then the droplet easily rewets the microchip and the binding site, causing the microchip to return to its aligned position.

#### 4.1.2 Compression

Based on the static height of the droplet  $z_0$ , the vertical restoring force  $F_z$  and the self-alignment of the microchip with the binding site associated with the compression  $\Delta z$  of the microchip (see Fig.3) are then explored. If a compression force is applied continuously to the microchip, the extrusion of the droplet will increase the contact angle. At last, the droplet may flow outside the microchip or the binding site and decrease the vertical restoring force  $F_z$ .

As presented in Fig.7, as the compression  $\Delta z$  increases, the vertical restoring force increases because the contact angle increases. As the droplet continues to be compressed, as shown in Fig.8, it even overflows outside the microchip or the binding site, and the vertical restoring force decreases drastically. After this moment, the microchip can no longer recover to the ideal alignment and the self-alignment of the microchip with the binding site becomes inaccurate. This phenomenon occurs as the compression  $\Delta z$  exceeds  $0.59\mu\text{m}$ ,  $1.95\mu\text{m}$  and  $4.38\mu\text{m}$  when the volume of the droplet is 12nl, 23nl and 35nl, respectively. The critical compression  $\Delta z_c$  is at most 3.15%, 5.42% and 7.98% of the static height of droplet  $z_0$ , as presented in Fig.7.

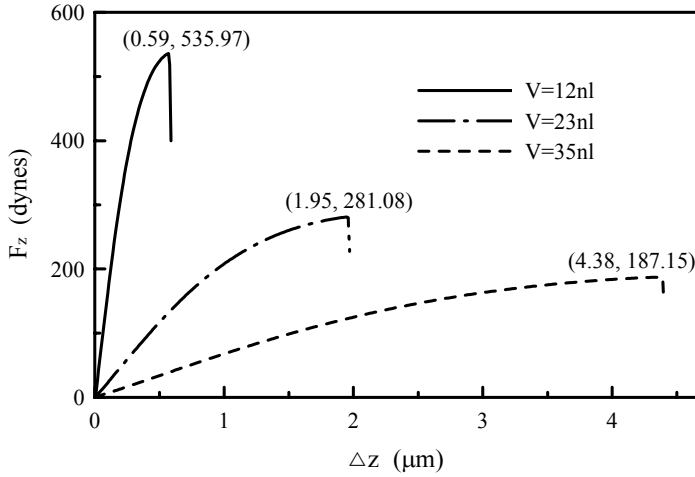


Figure 7: The calculated vertical restoring force  $F_z$  versus the compression  $\Delta z$

#### 4.1.3 Yawing

Based on the static height of the droplet  $z_0$ , the restoring torque and the self-alignment of the microchip with the binding site associated with the yawing angle  $\Delta\phi_1$  of the microchip (see Fig.3) are explored. As displayed in Fig.9, as the initial angle of yawing  $\Delta\phi_1$  increases, the restoring torque  $\tau$  increases. As presented in Fig.10, a higher yawing angle  $\Delta\phi_1$  causes the contact line to move farther away from the corners of the microchip and the binding site. As the area of overlap of the microchip and the binding site becomes smaller, the droplet tends to flow around the outside of the microchip. As yawing angle  $\Delta\phi_1$  increases to its critical value  $\Delta\phi_{1c}$ , the restoring torque  $\tau$  also reaches its maximum. Before the restoring torque  $\tau$  reaches its maximum, the microchip can be restored to its aligned position. However, when the yawing angle  $\Delta\phi_1$  exceeds its critical value  $\Delta\phi_{1c}$ , the microchip cannot align accurately with the binding site. It is worthwhile to note that the permitted yawing angle  $\Delta\phi_1$  will be constrained by the volume of the droplet. When the volume of the droplet is 12nl, 23nl and 35nl, the critical yawing angle  $\Delta\phi_{1c}$  of the microchip in the present study is found as  $8.78^\circ$ ,  $14.68^\circ$  and  $20.67^\circ$  respectively. The three-dimensional deformation of the droplet with a volume of 35nl at the critical yawing angle  $\Delta\phi_1=20.67^\circ$  is also displayed in Fig.10. In Fig.11, the dashed line represents the sides of the microchip or the binding site. The gray area and the solid line on the microchip or the binding site represent the contact line and the contact area calculated by the Surface Evolver Program. As the yawing angle  $\Delta\phi_1$  increases, the contact line moves farther away from the corners of the microchip or

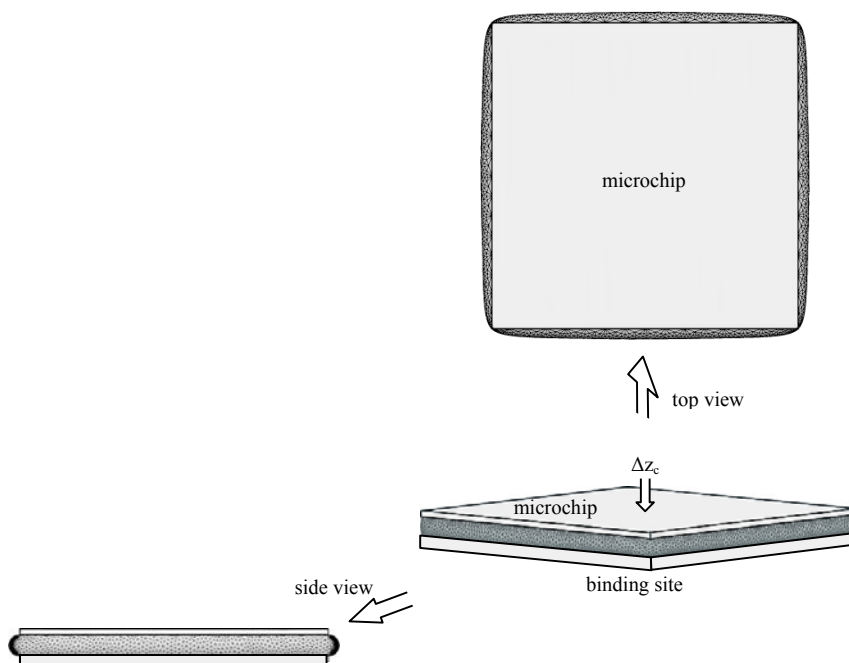


Figure 8: The overflow of the droplet at the critical compression  $\Delta z_c = 4.38 \mu\text{m}$  ( $V = 35 \text{nl}$ )

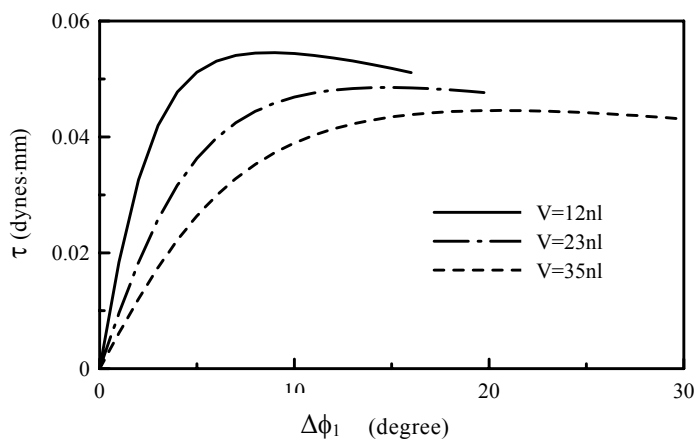


Figure 9: he calculated restoring torque  $\tau$  versus the yawing angle  $\Delta\phi_1$

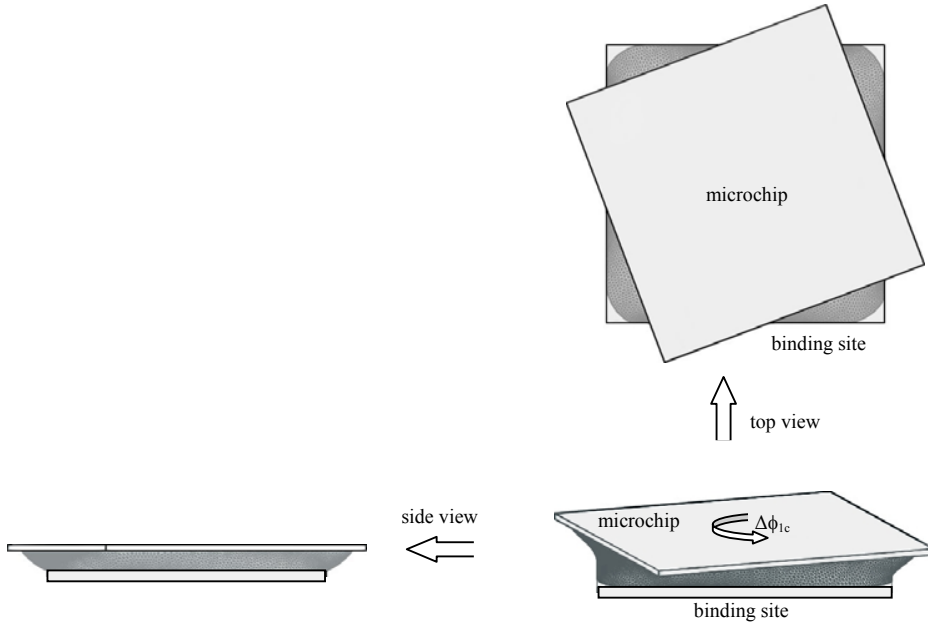


Figure 10: The deformation of the droplet at the critical yawing angle  $\Delta\phi_{1c}=20.67^\circ$  ( $V=35$  nl)

the binding site.

#### 4.1.4 Rolling

The restoring torque and the self-alignment of the microchip with the binding site are analyzed when the microchip is at the rolling angle  $\Delta\phi_2$ . Fig.12 reveals that as the rolling angle  $\Delta\phi_2$  increases, the restoring torque  $\tau$  also increases, but the rate of increase falls slowly until the microchip touches the binding site. The allowable rolling angles for the contact between the microchip and the binding site on droplet of volume 12nl, 23nl and 35nl are  $1.9^\circ$ ,  $3.5^\circ$  and  $4.8^\circ$  (see Fig.13) respectively. As the volume of a droplet decreases, its static height  $z_0$  declines and the allowable rolling angle also becomes small. In considering example of the study, the allowance of the maximum rolling angle for the restoring self-alignment of the microchip is much smaller than other motions. Accordingly, it is extremely sensitive to the self-alignment of the microchip with the binding site.

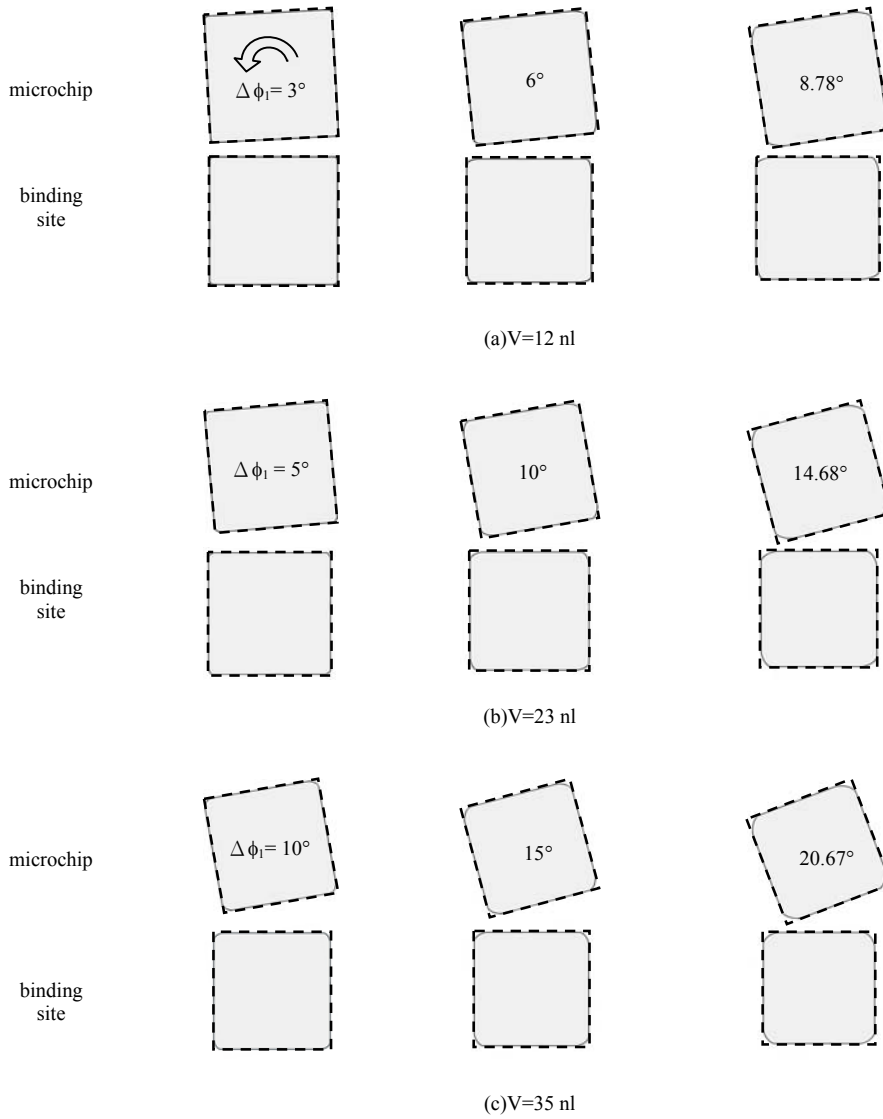


Figure 11: The contact line and the contact area on the microchip and the binding site at various yawing angles  $\Delta\phi_1$  of the microchip

#### 4.2 Triangular microchip and binding site

The analysis model proposed herein can be extended to other shapes of microchip or binding site. Another test example of the self-alignment of a triangular microchip



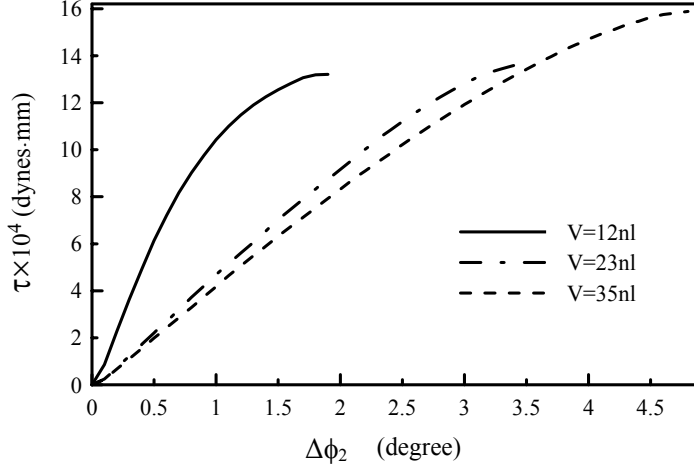


Figure 12: The calculated restoring torque  $\tau$  versus the rolling angle  $\Delta\phi_2$

with a binding site is considered (Sato *et al.*, 2003). The length of each side of the triangular microchip and the binding site is  $780\mu\text{m}$  with the thickness  $15\mu\text{m}$ . Since the experiment performed by Sato *et al.* (2003) did not provide the volume of the droplet or the weight of the microchip, the same weight of the microchip and the volume of the droplet 12nl as applied in the above case are assumed here. Calculations made using the Surface Evolver Program yield a static height of the droplet  $z_0$  of  $45\mu\text{m}$ . As indicated in Fig.14, Sato *et al.* (2003) found that when the microchip has an acute angle of corner, overflow occurs along the sides and no wet area is observed at corners. Fig.15 displays the magnified images for the corresponding locations by the present computation using the Surface Evolver Program, which agrees closely with the experimental results of Sato *et al.* (2003).

## 5 Concluding remarks

Using the Surface Evolver Program, this study has successfully established a three-dimensional analysis model, which accurately describes the self-alignment of the microchip with the binding site under the motions, including translation, compression, yawing and rolling. The effects of the droplet surface tension, droplet volume and wettability of interfaces, are considered. The contact characteristics between the droplet and the microchip/binding site, such as the contact line, contact area, overflow and no wet area, are thus drawn in details. The critical restoring force or restoring torque induced on the microchip under those motions can be accurately

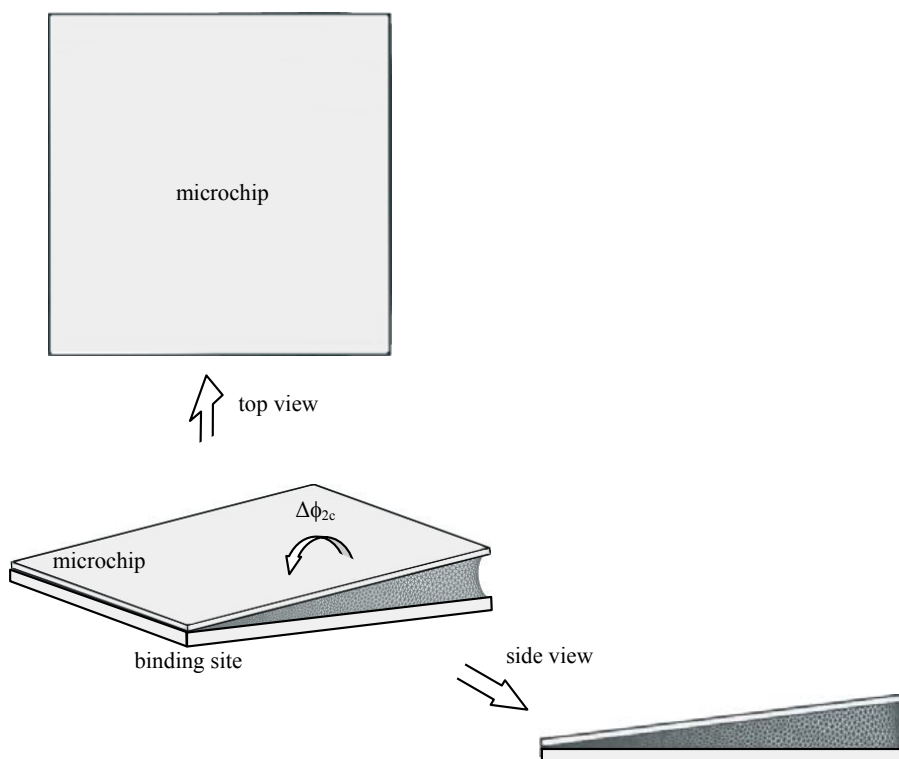


Figure 13: The deformation of the droplet at the allowable rolling angle  $\Delta\phi_{2c}=4.8^\circ$  ( $V=35$  nl)

determined. Therefore, the microchip can return to the position to be aligned on the movements under their critical values. The efforts can be practically applied to predict the self-alignment of the microchip with the binding sites in the electronic packaging for micro-electronic-mechanical systems.

The present three-dimensional analysis model can also be extended to deal with the self-alignment of the microchip with the binding site in aqueous solution and will be presented in a subsequent report.

**Acknowledgement:** The authors are grateful to the National Science Council, Taiwan, R.O.C., for financially supporting this research under grants NSC-98-2221-E-007-017-MY3. The authors would also like to express their thanks to Professor Ken Brakke, Susquehanna University, for his many useful discussions and

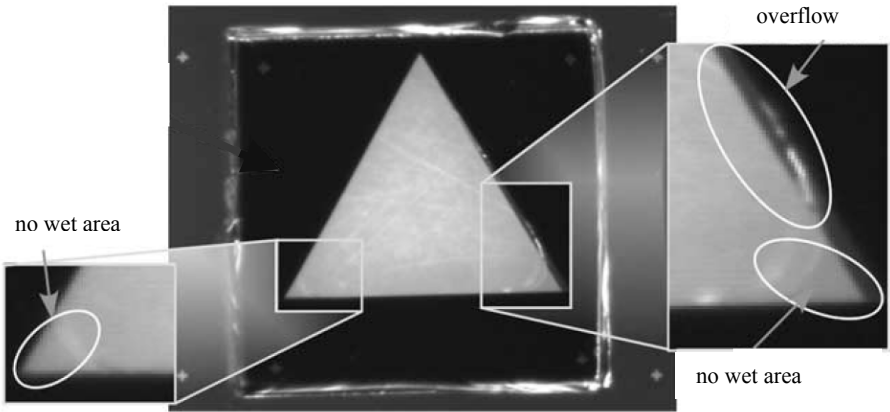


Figure 14: Overflow and no wet area in Sato's experiment (2003)

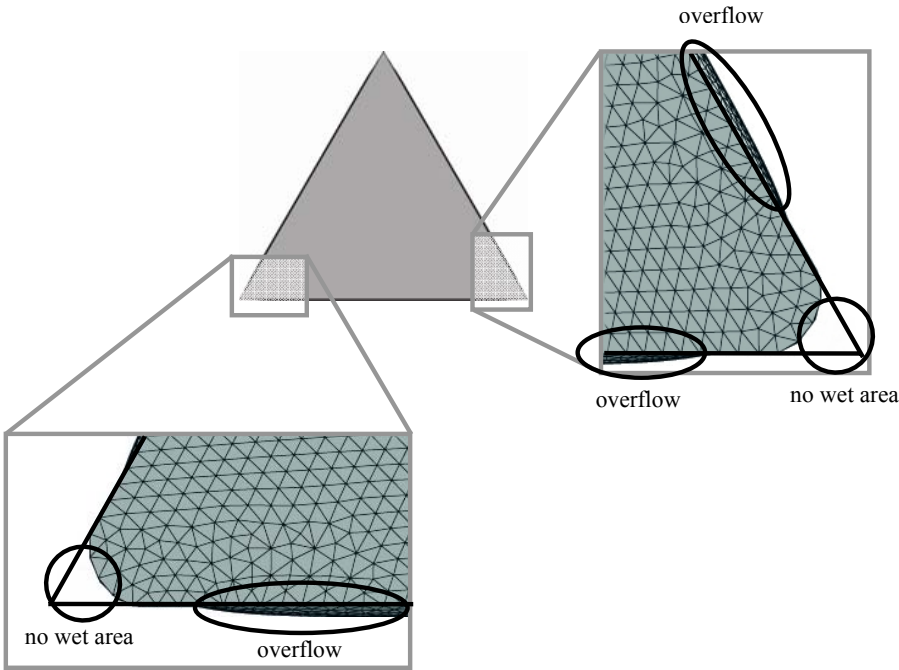


Figure 15: The present calculation of overflow and no wet area

suggestions for the Surface Evolver Program.

## References

- Berthier, J.; Brakke, K. A.; Grossi, F.; Sanchez, L.; Di Cioccio, L.** (2010): Self-Alignment of Silicon Chips on Wafers: A Capillary Approach. *Journal of Applied Physics*, vol.108, no.5, pp.054905-1–10.
- Böhringer, K. F.; Srinivasan, U.; Howe, R. T.** (2001): Modeling of Capillary Forces and Binding Sites for Fluidic Self-Assembly. *Proceedings of the IEEE Micro Electro Mechanical Systems (MEMS)*, pp.369–374.
- Brakke, K. A.** (1996): *Surface Evolver Manual*, Version 2.01. The Geometry Center. University of Minnesota.
- Chen, W. H.; Lin, S. R.; Chiang, K. N.** (2005): Stability of Solder Bridging for Area Array Type Packaging. *CMC: Computers, Materials, & Continua*, vol.2, no.3, pp.151–162.
- Elnaïem, H.; Casimir D.; Misra, P.; Gatica, S. M.** (2009): Nanobubbles at Water-Solid Interfaces: Calculation of the Contact Angle Based on a Simple Model. *CMC: Computers, Materials, & Continua*, vol.14, no.1, pp.23–34.
- Greiner, A.; Lienemann, J.; Korvink, J. G.; Xiong, X.; Hanein, Y.; Böhringer, K. F.** (2002): Capillary Forces in Micro-Fluidic Self-Assembly. *2002 International Conference on Modeling and Simulation of Microsystems - MSM 2002*, pp.198–201.
- Kim, J.-M.; Shin, Y. E.; Fujimoto, K.** (2004): Dynamic Modeling for Resin Self-Alignment Mechanism. *Microelectronics Reliability*, vol.44, no.6, pp.983–992.
- Kim, J.-M.; Yasuda, K.; Fujimoto, K.** (2005): Resin Self-Alignment Processes for Self-Assembly Systems. *Journal of Electronic Packaging, Transactions of the ASME*, vol.127, no.1, pp.18–24.
- Lin, H. C.; Kung, C.; Chen, R. S.** (2007): Evaluations of the BGA Solder Ball Shape by Using Energy Method. *CMC: Computers, Materials, & Continua*, vol.6, no.1, pp.43–50.
- Lo, J. C. C.; Lee, S. W. R.; Wu, H. H. L.; Lam, J. K. S.** (2008): Determination of Solder Bump Stand-off Height in a Flip-Chip Sub-Mount for Micro-Opto-Electro-Mechanical System (MOEMS) Packaging Applications. *Proceedings - Electronic Components and Technology Conference*, pp. 1887–1892.
- Myers, D.** (1999): *Surfaces, Interfaces, and Colloids*, second ed., John Wiley & Sons, New York.
- Sato, K.; Hata, S.; Shimokohbe, A.** (1999): Self-Alignment of Microparts Using Water Surface Tension. *Proceedings of SPIE - The International Society for Optical*

*Engineering*, vol.3892, pp.321–329.

**Sato, K.; Ito, K.; Hata, S.; Shimokohbe, A.** (2003): Self-Alignment of Microparts Using Liquid Surface Tension - Behavior of Micropart and Alignment Characteristics. *Precision Engineering*, vol.27, no.1, pp.42–50.

**Srinivasan, U.; Howe, R. T.; Lieppriann, D.** (2001): Microstructure to Substrate Self-Assembly Using Capillary Forces. *Journal of Microelectromechanical Systems*, vol.10, no.1, pp.17–24.

**Tsai, C. G.; Hsieh, C. M.; Yeh J. A.** (2007): Self-Alignment of Microchips Using Surface Tension and Solid Edge. *Sensors and Actuators A: Physical*, vol.139, no.1–2, pp.343–349.

**Xie, H.; Koshizuka, S.; Oka, Y.** (2007): Modeling the Wetting Effects in Droplet Impingement using Particle Method. *CMES-Computer Modeling in Engineering & Sciences*, vol. 18, no. 1, pp.1–16.

**Yang, J. T.; Chen, J. C.; Huang, K. J.; Yeh, J. A.** (2006): Droplet manipulation on a hydrophobic textured surface with roughened patterns. *Journal of Microelectromechanical Systems*, vol. 15, no. 3, pp.697–707.

**Zhu, Q.; Wang, G.; Luo, L.** (1998): Optimization of Design and Manufacturing Parameters for Solder Joint Geometry and Self-Alignment in Flip-Chip Technology. *International Conference on Solid-State and Integrated Circuit Technology Proceedings*, pp.554–558.

